Colloid Surface Chemistry Critically Affects Multiple Particle Tracking Measurements of Biomaterials

M. T. Valentine,* Z. E. Perlman,[†‡] M. L. Gardel,* J. H. Shin,[§] P. Matsudaira,[¶] T. J. Mitchison,[†] and D. A. Weitz*

*Department of Physics and Division of Engineering and Applied Sciences, Harvard University, Cambridge, Massachusetts 02138; [†]Department of Cell Biology and Institute of Chemistry and Cell Biology, Harvard Medical School, Boston, Massachusetts 02115; [‡]Program in Biophysics, Harvard University, Cambridge, Massachusetts 02138; [§]Department of Mechanical Engineering, Massachusetts Institute of Technology, Cambridge, Massachusetts 02142; and [¶]Department of Biology, Massachusetts Institute of Technology and the Whitehead Institute for Biomedical Research, Cambridge, Massachusetts 02142

ABSTRACT Characterization of the properties of complex biomaterials using microrheological techniques has the promise of providing fundamental insights into their biomechanical functions; however, precise interpretations of such measurements are hindered by inadequate characterization of the interactions between tracers and the networks they probe. We here show that colloid surface chemistry can profoundly affect multiple particle tracking measurements of networks of fibrin, entangled F-actin solutions, and networks of cross-linked F-actin. We present a simple protocol to render the surface of colloidal probe particles protein-resistant by grafting short amine-terminated methoxy-poly(ethylene glycol) to the surface of carboxylated microspheres. We demonstrate that these poly(ethylene glycol)-coated tracers adsorb significantly less protein than particles coated with bovine serum albumin or unmodified probe particles. We establish that varying particle surface chemistry selectively tunes the sensitivity of the particles to different physical properties of their microenvironments. Specifically, particles that are weakly bound to a heterogeneous network are sensitive to changes in network stiffness, whereas protein-resistant tracers measure changes in the viscosity of the fluid and in the network microstructure. We demonstrate experimentally that two-particle microrheology analysis significantly reduces differences arising from tracer surface chemistry, indicating that modifications of network properties near the particle do not introduce large-scale heterogeneities. Our results establish that controlling colloid-protein interactions is crucial to the successful application of multiple particle tracking techniques to reconstituted protein networks, cytoplasm, and cells.

INTRODUCTION

Understanding the unique microscopic mechanical properties of biopolymer networks is essential to understanding their biological function. For example, fibrin networks assemble at wounds and provide the critical scaffolding upon which healing and tissue repair occur, and actin networks in the cytoskeleton guide cell shape, motility, and division (Clark, 2001; Howard, 2001; Boal, 2002). The mechanical properties of networks such as these are determined by structures and dynamics on the scale of microns, and so precise tools to probe network response on these length scales are required. As a result, microrheology techniques have been developed to measure the microscopic viscoelastic and mechanical properties of soft materials by analyzing the motion of embedded tracers driven by thermal (Mason and Weitz, 1995; Gittes et al., 1997; Mason et al., 1997a,b), magnetic (Amblard et al., 1996b; Schmidt et al., 1996; Ziemann et al., 1994), or optical forces (Valentine et al., 1996; Hough and Ou-Yang, 1999). In these measurements, tracer displacements are sensitive to local viscous and elastic forces, as well as chemical and steric interactions between the particle and network. This provides the opportunity to probe many aspects of complex biomaterials; however, because the details of network architecture and molecular composition are often not known a priori, these multiple sensitivities can also lead to ambiguities in the interpretation of these data.

In one simplifying limit, when the chemical interactions between the tracers and polymers are negligible, it is possible to characterize tracer motions based only on the size of the probe relative to the native structural sizes of the network. Varying probe diameter with respect to these native lengths gives qualitatively different information about network mechanics. When thermally driven embedded probe particles are large compared to all structural length scales, as illustrated in the sketch in Fig. 1 *A*, the ensemble-averaged mean-squared displacement (MSD) is directly related to the linear frequency-dependent viscous and elastic moduli using a generalized Stokes-Einstein relation (Mason and Weitz, 1995; Gittes et al., 1997; Mason et al., 1997a,b; Dasgupta et al., 2002). By contrast, when the embedded particles are approximately equal to or smaller than the structural length scales of the material, as sketched in Fig. 1 *B*, particles move within small, mechanically distinct microenvironments and their dynamics are no longer directly related to the bulk viscoelastic response (Valentine et al., 2001; Wong et al., 2004). Rather, their Brownian movements are sensitive to the viscosity of the solvent, the effects of macromolecular

Submitted November 29, 2003, and accepted for publication February 23, 2004.

Address reprint requests to Prof. David A Weitz, Physics Department, Harvard University, 29 Oxford St., Cambridge, MA 02138. Tel.: 617-496-2842; E-mail: weitz@deas.harvard.edu.

0006-3495/04/06/4004/11 $2.00

doi: 10.1529/biophysj.103.037812

crowding, and steric and hydrodynamic interactions with the network (Jones and Luby-Phelps, 1996; Luby-Phelps, 2000; Chen et al., 2003). Since many biopolymer networks are structured on micron length scales, measurements can be extremely sensitive to even small changes in the tracer diameter or the mesh size of the network. Careful studies of tracer displacements as a function of probe size are thus often required.

In general, chemical interactions between tracers and protein networks cannot be ignored and introduce large ambiguities in the interpretation of network responses. Thus, the ability to characterize and modify surface interactions, as well as tracer size, is crucial to proper interpretation of measurements of complex biomaterials. For microrheology measurements of network viscoelasticity for example, the particles must not only be large in comparison to all structural length scales, but must also be sufficiently resistant to protein adsorption to prevent the local modification of network architecture and introduction of small heterogeneities. Alternatively, for measurements of the microenvironments of a heterogeneous material with tracers that are smaller than the structural length scales, even a small amount of protein adsorption can cause particles to adhere to cavity walls, preventing them from fully exploring small pores and possibly even inducing local changes in network structure, leading to uncertainties in the interpretation of particle dynamics, as sketched in Fig. 1, *C* and *D*.

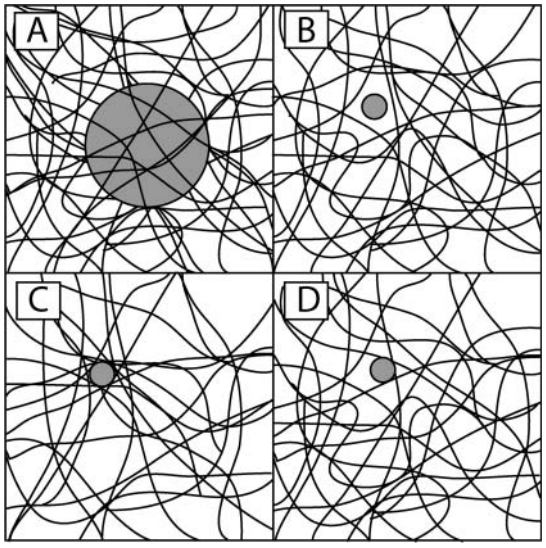

FIGURE 1 Sketch illustrating several physical scenarios for the way colloidal particles can be embedded in a biopolymer network. (*A*) When chemically inert particles of radius $a \gg$ network mesh size ξ are used, the mean-squared displacement is directly related to the linear viscoelastic moduli. (*B*) When particles are resistant to protein adsorption and $a \leq \xi$, tracers move within small microenvironments and their movements are sensitive to the viscosity of the solvent and hydrodynamic interactions with the network, but do not reflect the bulk viscoelasticity. (*C*) For $a \leq \xi$, ''sticky'' tracers adsorb protein and recruit polymer strands to their surface, possibly modifying the local polymer concentration near the sphere. In this case, particle movements do reflect network fluctuations; however, the tracers may sample unusually and artifactually stiff regions of the network, leading to uncertainty in the interpretation of relationship of the particle dynamics to the network dynamics. (*D*) For $a \leq \xi$, even a small amount of protein adsorption can cause particles to adhere to cavity walls, leading to unusual hydrodynamic interactions with the adsorbed network, and uncertainty in the interpretation of these data.

One approach that has been developed to address some of these limitations is two-particle microrheology, in which the correlated motion of pairs of particles is analyzed to measure the long wavelength deformation of a network (Crocker et al., 2000; Levine and Lubensky, 2000). Correlated motions arise only from fluctuations on length scales greater than the interparticle separation distance; thus two-particle microrheology is insensitive to local heterogeneities and promises to be independent of the coupling of the particle to the medium. The ability to isolate the long wavelength network response is a significant advance. However to fully characterize the microscopic properties of complex materials, the ability to probe network mechanics at the length scale of the particle is desirable. Therefore, a full study of the effect of particle surface chemistry on tracer movements in biopolymer gels is required.

Ideally, it would be possible to tune tracer surface chemistry to prevent undesirable protein adsorption yet allow specific and controllable binding; however, such surfaces are not commercially available, and studies of the effect of protein binding on particle mobility are limited. Designing tracers with tunable adsorption properties requires knowledge of the extremely complex and poorly understood microscopic surface interactions between colloids and proteins (Haynes and Norde, 1994). Since the molecular level details are unknown, one common approach to reduce the nonspecific adsorption of a particular protein is to simply preincubate the colloids with another protein solution that is known to have a high surface affinity, such as bovine serum albumin (BSA), to physically block any available protein binding sites. Protein coatings such as these have been shown to reduce the adsorption of some proteins to colloidal surfaces, and in many cases BSA-coated particles provide an excellent alternative to bare tracers. For example, previous measurements have demonstrated that BSA-coated particles are more mobile than bare carboxylate-modified latex (CML) spheres when used in micromechanical measurements of cross-linked networks of actin; however, the adsorbed BSA monolayer is patchy and does not render the particles completely resistant to additional protein adsorption (McGrath et al., 2000). Moreover, because the protein layer is simply adsorbed, and not covalently bound, some desorption of the BSA from the surface is possible, complicating interpretations of particle dynamics (McGrath et al., 2000).

As an alternative to BSA coating, a dense monolayer of poly(ethylene glycol) (PEG) has been shown empirically to

reduce the adsorption of a wide variety of proteins when grafted onto flat surfaces (Prime and Whitesides, 1991, 1993; Ostuni et al., 2001; Harder et al., 1998). The origin of protein resistance in PEG-coated surfaces is generally attributed to steric repulsion effects arising from both the loss of conformational entropy of the polymer as the brush is compressed and the disfavorable desolvation of the chains as water molecules are expelled from the polymer layer (de Gennes, 1987; Jeon et al., 1991; Grunze et al., 1998). Despite the success of PEG-coated flat surfaces, the adsorption properties of alternative geometries have not been fully explored, as PEG-coated colloidal particles are not readily available commercially and are not widely used (Weisbecker et al., 1996; Liu et al., 1997; Shay et al., 2000, 2001; De Sousa Delgado et al., 2001; McGrath et al., 2003).

In this article, we develop a simple and robust protocol to graft short amine-terminated methoxy-poly(ethylene glycol) to the surface of carboxylate-modified colloids using commercially available reagents. We demonstrate that PEG-coated colloids adsorb significantly less protein than bare CML spheres or probes coated with physisorbed BSA, and use multiple particle tracking techniques to measure the Brownian movements of these tracers embedded in biopolymer networks. We choose three protein systems that display different adsorption characteristics and whose mechanical properties are critical to their biological function. We first choose fibrinogen, a globular protein that has a very strong surface affinity and is thus commonly used to investigate protein-surface interactions (Prime and Whitesides, 1993; Harder et al., 1998; Lahiri et al., 1999; Alcantar et al., 2000; Chapman et al., 2000; Ostuni et al., 2001; Valiokas et al., 2001; Chirakul et al., 2002). Because fibrinogen is found in blood plasma and is involved in the formation of clots, characterizing and controlling its interactions with foreign surfaces in vivo is critical to the successful biomedical implantation of therapeutic devices and prostheses. In vitro, fibrinogen self-assembles into a cross-linked and branched semiflexible fibrin network upon activation by thrombin (Doolittle, 1981). The second sample is filamentous actin (F-actin), a well-studied and important semiflexible biopolymer that is found in cellular cytoplasm and plays an essential role in determining the strength and shape of living cells (Maggs, 1997a,b; Morse, 1998; Gittes and Mackintosh, 1998; Howard, 2001; Alberts et al., 2002; Boal, 2002). Reconstituted F-actin networks have been studied extensively with microrheology techniques, and understanding and controlling the surface interactions of F-actin with colloids is imperative for properly interpreting those data (Ziemann et al., 1994, Amblard et al., 1996a, Schmidt et al., 1996, McGrath et al., 2000; Keller et al. 2001, Gardel et al., 2003). The final sample, a composite protein network composed of F-actin and the actin-bundling protein scruin, is chosen to investigate the effect of surface interactions in networks that more closely approximate physiologically relevant actin gels, which are typically cross-linked or bundled by actin-binding proteins in vivo.

With these measurements, we demonstrate that, by varying particle surface modifications, we can selectively tune the sensitivity of the particles to the different physical properties of the biomaterials they probe. In particular, we find that particles that are weakly bound to a heterogeneous network are sensitive to changes in local stiffness, whereas the protein resistant PEG-coated tracers are sensitive to changes in viscosity and microstructure. Additionally, we provide an experimental demonstration that local variations in network mechanics introduced by protein adsorption are uncorrelated over large distances, and thus two-particle microrheology essentially eliminates the differences due to surface chemistry effects.

MATERIALS AND METHODS

Preparing PEG-coated particles

To create the PEG-coated particles, we attach amine-terminated methoxy-poly(ethylene glycol), (mPEG-NH_2), NH_2-$(CH_2$-CH_2-$O)_n$-OCH_3, where, on average, $n = 16$, resulting in an average molecular mass of 750 Da (Rapp Polymere, Tübingen, Germany), to CML particles (Molecular Probes, Eugene, OR, or Interfacial Dynamics, Portland, OR) using standard carbodiimide coupling chemistry. In this reaction, the carboxylic acids are activated by the formation at low pH of a reactive *N*-hydroxysuccinimide (NHS) ester, proceeding through the formation of a less stable ester with 1-[3-(dimethylamino)propyl]-3-ethylcarbodiimide (EDC) (Sigma-Aldrich, St. Louis, MO). The activated esters are then mixed with mPEG-NH_2 at higher pH to accelerate deprotonation of the amine, which reacts with the NHS-ester to yield a stable amide bond.

To minimize the probability of colloidal aggregation, we perform all buffer exchanges slowly using dialysis tubing, rather than the more traditional centrifugation or filtration techniques. Also, we foreshorten the timing of the low-pH ester formation step, since we observe significant aggregation when this reaction is allowed to proceed for >30 min, which we attribute to the loss of electrostatic repulsion. All reactions and washes are performed under constant slow stirring, and with the buffer volume exceeding the particle solution volume at least 100-fold.

Spheres are loaded into dialysis tubing (SpectraPor, 10 kD cutoff; Spectrum, Rancho Dominguez, CA) at number densities of $\sim 10^{11}$–10^{13} particles/mL; we observe that higher number densities result in aggregation and poor coupling efficiency. The bags are submerged in MES buffer (100 mM 2-(*N*-morpholino)ethanesulfonic acid) at pH 6.0 for 2 h. The bags are then rinsed with deionized (DI) water and submerged in a solution containing 15 mM EDC, 5 mM NHS, and a 10-fold excess of mPEG-NH_2 in MES buffer for 30 min. Both the EDC and NHS are in vast excess, so the concentrations may be varied slightly without loss of coupling efficiency; however, using significantly higher concentrations of either reagent may accelerate the loss of charge stability and promote aggregation. The mPEG-NH_2 is added at this step primarily to ensure its immediate presence in the dialysis bag after the pH is raised; a 100-fold increase in concentration has no effect on the reaction efficiency or protein resistivity of the particles.

The bags are then submerged into borate buffer (50 mM boric acid, 36 mM sodium tetraborate) at pH 8.5, with NHS and mPEG-NH_2 at the same concentrations as above. The reaction is allowed to proceed for at least 8 h under constant gentle stirring, and is repeated twice with fresh buffer and reagents. After the third reaction, the particles are washed in pure borate buffer for at least 2 h to remove any unreacted reagents and polymer. The particles are then recovered and stored at 4°C; they remain stable against aggregation and protein-resistant for at least several months.

Preparation of BSA-coated particles

Bovine serum albumin (Sigma-Aldrich) is slowly dissolved in phosphate buffered saline (PBS) (Gibco, Invitrogen Life Technologies, Carlsbad, CA) at room temperature at concentrations of 5 mg/mL. CML particles, with diameters of either 1.0 μm or 0.84 μm, are incubated with the BSA solutions for 1 h at room temperature, or overnight at 4°C. The suspensions are centrifuged at low speed for 30 min, the supernatant is discarded, and the particles are resuspended in fresh PBS. This washing is repeated three or more times to remove any unbound BSA. Particles are stored at 4°C and used within 48 h of preparation, to reduce the likelihood of the BSA desorbing from the particle surface.

Characterization of protein adsorption using fluorescent BSA

Undyed particles of each surface chemistry are incubated with bovine-derived albumin, labeled with tetramethylrhodamine isothiocyanate (R-BSA) (Sigma-Aldrich), then observed with fluorescence microscopy to determine the amount of protein adsorption. The R-BSA is dissolved in PBS at a concentration of 1 mg/mL and stored at 4°C for up to 48 h. For each of the differently treated particles, we add 50 μL of 0.84 μm particles at a volume fraction of ~0.3% to 500 μL of the R-BSA solution and incubate the solution overnight at 4°C under constant slow rotation. Volume fractions of the BSA- and PEG-coated particles are determined by visually comparing the diluted particle suspensions with optical microscopy to solutions of CML particles at known volume fractions. The suspensions are then centrifuged at low speed for 30 min, the supernatant is discarded, and the particles are resuspended in fresh PBS. This washing is repeated three or more times to remove any unbound R-BSA. Particles are observed with a Leica DM-IRB inverted microscope with a 100× magnification, oil-immersion objective, with numerical aperture 1.4. Using Metamorph acquisition software (Universal Imaging, Downingtown, PA), bright-field images are obtained with a Hamamatsu C2400 charge-coupled device (CCD) camera, and fluorescence images are obtained using a Hamamatsu EB-CCD intensified camera (Hamamatsu, Bridgewater, NJ). Images are analyzed using Adobe Photoshop.

Multiple particle tracking

For visualization of particle dynamics, samples are loaded into microscope observation chambers that consist of three 1-mm spacers that are positioned in a ''U'' shape and sandwiched between a glass slide and a No. 1.5 glass cover slip. The slide and cover slip are rinsed with water and methanol, and air dried before use. All pieces are held in place with ultraviolet-cured optical glue (No. 81 or No. 61, Norland, Cranbury, NJ). To reduce the amount of nonspecific protein adsorption onto the glass surfaces, a 5 mg/mL BSA solution is loaded into the chamber and incubated at room temperature for at least 1 h before use. After incubation, the chambers are rinsed exhaustively with DI water to remove any remaining unbound BSA and the chambers are air-dried before use. Sample volumes of 30–50 μL are loaded into the observation chambers, and the open side is sealed with high vacuum grease to prevent evaporation. Care is taken to prevent any air bubbles from contacting the sample as such bubbles can lead to slow leakage and contribute to macroscopic drift of the embedded particles. Once loaded, the chamber is left undisturbed for at least 30 min at room temperature to allow the protein networks to form. We observe no differences in particle dynamics for waiting times of 60 min or more, suggesting that the micromechanical properties of the sample have reached a steady state during this time. The slides are then gently transferred to an inverted research microscope (Leica DM-IRB) for observation. For two-particle microrheology measurements, we image at least 100 microns into the sample to minimize hydrodynamic interactions with the walls.

Particles are imaged with bright-field or epifluorescence microscopy, and the particle movements are recorded with a CCD camera (Cohu Electronics, San Diego, CA) onto S-VHS videotape or are directly digitized in real-time using custom-written image analysis software (Keller et al., 2001). Video frames are acquired to obtain tracer positions with 30 Hz temporal resolution. In each frame, the positions of the particles are identified by finding the brightness-averaged centroid position with a subpixel accuracy of ~10–20 nm (Crocker and Grier, 1996). Positions are then linked in time to create two-dimensional particle trajectories.

One-particle microrheology

To measure network viscoelasticity, we embed small colloidal particles into a complex fluid, record their thermally activated Brownian motions, and calculate the ensemble averaged MSD, $\langle \Delta x^2(\tau) \rangle = \langle |x(t+\tau) - x(t)|^2 \rangle$, as a function of lag time, τ, where the angled brackets indicate an average over many starting times t and the ensemble of particles in the field of view. For spherical tracers that are embedded in a homogeneous and incompressible medium, the MSD is directly related to the viscoelastic response of the surrounding material (Mason and Weitz, 1995; Gittes et al., 1997; Mason et al., 1997a,b; Levine and Lubensky, 2000). Physically, this can be understood by considering two limiting cases: a purely viscous fluid and a completely elastic solid. For a purely viscous fluid, the d-dimensional MSD will increase linearly with lag time $\langle \Delta x^2(\tau) \rangle = 2dD\tau$. The viscosity $\eta = k_B T/6\pi Da$ can be calculated from the diffusion coefficient D, where a is the particle radius. For a purely elastic material, the MSD will reach an average plateau value $\langle \Delta x_p^2 \rangle$ that is independent of lag time and is determined by the elastic modulus of the material. Equating the thermal energy to the elastic deformation energy, we estimate the elastic plateau modulus $G_p \sim k_B T/\langle \Delta x_p^2 \rangle a$. In general, the full frequency dependence of the viscoelastic moduli can be obtained from the MSD using a generalized Stokes-Einstein equation: $\tilde{x}^2(s) = k_B T/\pi s a \tilde{G}(s)$, where $\tilde{x}^2(s)$ is the Laplace transform of $\langle \Delta x^2(\tau) \rangle$, and $\tilde{G}(s)$ is the viscoelastic response as a function of the Laplace frequency s (Mason and Weitz, 1995; Mason et al., 1997a,b). However, many biological materials have heterogeneities on micron length scales, due to native microstructure or irregularities introduced by the inclusion of small colloids, which preclude the application of one-particle microrheology.

Two-particle microrheology

Two-particle microrheology uses the correlated movements of pairs of separated particles to measure the long-wavelength macroscopic response of materials that are inhomogeneous on the length scale of a single tracer but homogeneous on the length scale of several particles (Crocker et al., 2000; Levine and Lubensky, 2000). We calculate the ensemble-averaged tensor product of the tracer displacements: $D_{\alpha\beta}(r,\tau) = \langle \Delta r_\alpha^i(t,\tau) \Delta r_\beta^j(t,\tau) \delta[r - R^{ij}(t)] \rangle_{i \neq j,t}$, where i and j label different particles, α and β label different coordinates, and R_{ij} is the distance between particles i and j. In the limit, $r \gg a$, for an incompressible medium, $D_{rr}(r,s) = k_B T/2\pi r s \tilde{G}(s)$, with no dependence on the particle size, shape, or boundary conditions. Using only the R_{ij} where $D_{rr} \sim 1/r$, to ensure that the medium can be treated as a coarse-grained homogeneous continuum, we extrapolate the correlated motion to the length scale a and define the two-particle mean-squared displacement $\langle \Delta r^2(\tau) \rangle_D = 2r/aD_{rr}(r,\tau)$.

Preparation of biopolymer gels

To form the fibrin network, fibrinogen monomers, at a concentration of 0.44 mg/mL, are rapidly thawed from −70°C, placed at room temperature, and used within 4 h. Concentrated thrombin is rapidly thawed from −70°C, stored on ice for up to 2 h, and diluted to 0.6 μM immediately before use. The network is formed by mixing 50 μL 0.44 mg/mL fibrinogen in Tris-buffered saline (145 mM NaCl, 20 mM Trizma base, 0.3 mM sodium azide, 0.01% Tween 20; pH = 7.4), 0.5 μL 1M $CaCl_2$, 0.5 μL of the particle solution, and 0.5 μL of 0.6 μM thrombin. Once the thrombin is added, the

fibrinogen solution quickly polymerizes to form the fibrin network, and must be transferred immediately into the measurement chamber to prevent mechanical disruption of the network due to pipetting.

To form the entangled F-actin networks, lyophilized globular actin (G-actin) is thawed from −20°C, dissolved in DI water, and dialyzed against fresh G-buffer (2 mM Tris HCl, 0.2 mM ATP, 0.2 mM $CaCl_2$, 0.2 mM dithiothreitol, 0.005% sodium azide) at pH 8.0 and 4°C for 24 h, during which time G-buffer is replaced every 8 h. Solutions of G-actin are kept at 4°C and used within 7 days of preparation. G-actin is mixed with the colloidal particle suspensions and fresh G-buffer to adjust final concentration. Polymerization is initiated by addition of 1/10 of the final sample volume of 10× F-buffer (20 mM Tris HCl, 20 mM $MgCl_2$, 1 M KCl, 2 mM dithiothreitol, 2 mM $CaCl_2$, 5 mM ATP, pH 7.5). Samples are mixed gently for 10 s, then loaded into observation chambers and allowed to equilibrate for 60 min at room temperature before particle movements are recorded.

To form composite F-actin gels, we use scruin, an actin-bundling protein found uniquely in the sperm of horseshoe crabs, where it bundles F-actin in the acrosome (Schmid et al., 1995; Tilney et al., 1996). Scruin purification is performed as described by Sun et al. (1997) with minor modifications (J. Shin, M. Gardel, L. Mahadevan, P. Matsudaira, and D. Weitz, unpublished). The integrity of the protein is checked by SDS-PAGE gel electrophoresis before each experiment to ensure low level of proteolysis or degradation. The concentrations are determined either by the Bradford assay, using BSA as a standard, or by absorbance at 280 nm (Bradford, 1976). Cross-linked and bundled actin networks are prepared by adding G-actin to the mixture of scruin, particles, and 10× F-buffer. Samples are allowed to equilibrate for 1 h before observation.

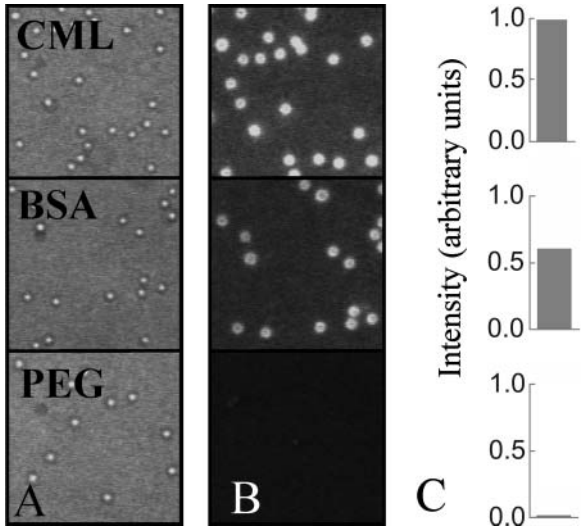

FIGURE 2 Bright-field (*A*) and fluorescence (*B*) images of 0.84-μm CML and BSA- and PEG-coated particles that have been incubated with R-BSA. The fluorescence intensity indicates the binding capacity of each particle. The CML and BSA-coated particles adsorb a significant amount of protein, whereas the adsorption on the PEG-coated particles is very small. There is a shift in the fields of view between the bright-field and fluorescence images due to different optics along the two paths; in some cases particles have diffused slightly between image acquisitions. (*C*) Normalized fluorescence intensity of the CML and BSA- and PEG-coated particles incubated with R-BSA. The intensity of the BSA-coated particles is 60% of that of the CML particles, indicating that the BSA coating does prevent some protein adsorption, but does not render the particles completely inert. The intensity of the PEG-coated particles is only 2% of that of the CML particles, indicating a significant improvement in protein resistivity.

RESULTS AND DISCUSSION

Determination of particle protein-binding capacity

To characterize the amount of protein adsorbed onto particles with different surface modifications, we incubate 0.84-μm undyed CML and BSA- and PEG-coated particles with bovine-derived albumin, labeled with rhodamine and observe the particles with bright-field and fluorescence microscopy. Since the particles are not inherently fluorescent, only those that have adsorbed a considerable amount of fluorescently labeled protein will be visible with fluorescence imaging. Bright-field images of particles are used to identify the positions of the tracers, as shown in Fig. 2 *A*. Both CML and BSA-coated particles fluoresce, indicating that these surface chemistries allow significant protein adsorption, as shown in Fig. 2 *B*. By contrast, the PEG-coated particles show negligible fluorescence, indicating that very little protein has adsorbed. To quantify the amount of adsorption, we calculate the relative fluorescence intensities of the particles by measuring the total intensity of the image, subtracting the average background intensity, which is measured in the absence of the particles, and normalizing by the number of particles in the field of view. The intensity of the BSA-coated particles is only 60% of the intensity of the CML particles, as shown in Fig. 2 *C*, indicating that the BSA coating does prevent some amount of additional protein adsorption, but does not render the particles completely inert. This partial reduction in adsorption is consistent with previous measurements of BSA coating on CML spheres, which indicate that even with coating solutions of up to 400 mg/mL BSA, the surface coverage of physisorbed BSA never exceeds 50% of the total particle surface area, and thus cannot completely prevent protein adsorption (McGrath et al., 2000). By contrast, the PEG-coated particles are significantly more protein resistant than either the CML or BSA-coated spheres; the intensity of the PEG-coated particles is only 2% of that of the untreated CML probes.

Mechanical properties of fibrin

To explore the effect of surface chemistry on particle mobility in a biopolymer network, we form a cross-linked network of fibrin, and record the movements of 1-μm CML and BSA- and PEG-coated particles embedded in the gel. The mesh size of the 0.43 mg/mL fibrin network is ~5–10 μm, significantly larger than the diameter of the tracers, as observed with fluorescence microscopy of networks formed with rhodamine-dyed fibrinogen (data not shown). Thus the network is heterogeneous on the scale of individual particles, and we observe significant variations in particle dynamics due to differences in tracer surface chemistry. The CML and BSA-coated particles are constrained and barely move, whereas the PEG-coated particles are much more mobile and

the shape of their trajectories suggests a random walk, as shown in Fig. 3.

To better quantify the particle motions, we calculate the one-dimensional MSD. In no cases do the CML and BSA-coated tracers move detectably, and the value of the MSD is a reflection only of our error in identifying particle centers. Because the mesh size is large compared to the tracer diameter, it is unlikely that the particles are merely constrained by the elastic mesh; rather, these data suggest that these protein-adsorbing probes are adhering to a stiff elastic material. Although we are unable to accurately determine the MSD of either the CML or BSA-coated particles, we are able to place an upper bound on the MSD; from the squared measurement error of the particle positions, we estimate $\langle \Delta x_p^2 \rangle \leq 4 \times 10^{-4}\ \mu m^2$. For particles moving in a heterogeneous network, characterized by an average mesh size ξ, we estimate the elastic plateau modulus to be $G_p \sim k_B T / \langle \Delta x_p^2 \rangle \xi$ (Krall and Weitz, 1998). Using our upper bound for the MSD and $\xi \sim 5\ \mu m$, we estimate $G_p \geq 5$ Pa. Because the fibrin gels form very rapidly upon addition of thrombin and are extremely fragile, we are unable to reproducibly load the gels into a traditional mechanical rheometer for comparison.

By contrast, the MSD of each PEG-coated particle is well above our resolution limit, and thus accurately reflects the local microenvironment surrounding the tracer. By examining the one-dimensional MSDs of 46 individual PEG-coated particles, we observe a variety of different behaviors, as shown in Fig. 4. To collect sufficient statistics on individual particles, we analyze the trajectories only of particles that remain in focus for at least 10 s. Of the 46 particles, 38 move diffusively for lag times up to 1 s, with MSDs increasing linearly in τ, suggesting that because the PEG-coated particles resist protein adsorption, most are nearly unperturbed by the surrounding polymer strands. Moreover, we measure no difference in the one-dimensional MSD obtained using displacement data collected along two orthogonal directions, indicating that particles are not sensitive to any mechanical anisotropy that may be present in the network. At longer lag times, the particle motion may be influenced by the network; however, because the PEG-coated particles are able to diffuse through the network and out of our focal volume, we are unable to measure the MSD of the tracers at these timescales.

To improve our statistical accuracy, we calculate the ensemble-averaged MSD of these 38 mobile PEG-coated particles, and use this to determine the local viscosity η within the pores. We measure $\eta = 1.7$ mPa-s, consistent with the viscosity of the buffer, which we independently measure to be $\sim$1 mPa-s; this small increase may be due to enhanced hydrodynamic drag as the particles move through the polymer network (Valentine et al., 2001; Jones and Luby-Phelps, 1996). The remaining eight particles move subdiffusively with some reaching a saturated plateau value at long lag times. For these particles, we are unable to distinguish experimentally between particles that are constrained due to a small amount of adsorption of fibrin, and particles that are not bound, but merely reside in an unusually dense region of the gel where the local mesh size is approximately equal to or smaller than the tracer. For all measurements, the network is heterogeneous on the length scale of the particles, and in no case do we measure the bulk rheological response.

Surface chemistry effects on the microrheology of entangled F-actin networks

To further explore the effect of surface chemistry on the protein adsorption and mobility of colloids in biomaterials, we measure the movements of 1.0-μm CML and BSA- and PEG-coated particles in an 11.9 μM entangled F-actin network. F-actin networks have been studied extensively with microrheology techniques (Ziemann et al., 1994; Amblard et al., 1996a; Schmidt et al., 1996; Keller et al., 2001; Gardel et al., 2003), and the surface chemistry effects of CML and BSA-coated particles in actin networks have been previously reported in detail (McGrath et al., 2000). Here, we calculate the ensemble-averaged MSD for the PEG-coated particles, and compare to those of the CML and BSA-coated particles. There is a measurable reduction in the plateau value of the MSD, $\langle \Delta x_p^2 \rangle$, of the untreated CML particles, by roughly a factor of 2, in comparison to that of the BSA- and PEG-coated particles, as shown in Fig. 5; this is in agreement with previous work (McGrath et al., 2000). This reduction may indicate that the CML particles are more tightly bound to the polymer network, or that by binding to actin filaments, the CML particles introduce local cross-linking that slightly increases the local elastic modulus.

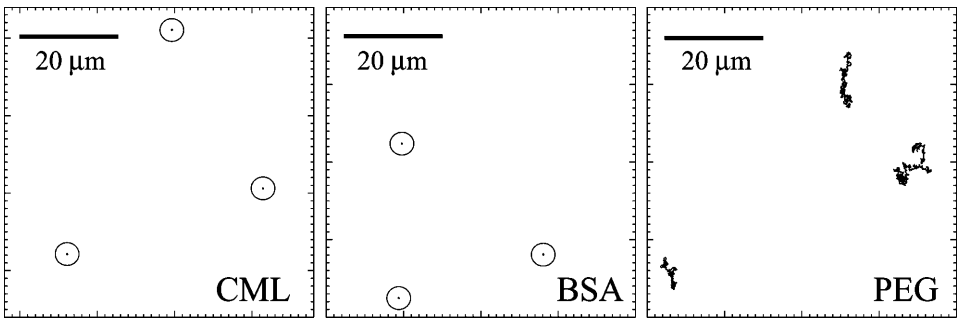

FIGURE 3 Trajectories of 1-μm CML and BSA- and PEG-coated particles in a 0.43 mg/mL fibrin network with $a/\xi \sim$ 0.1–0.2. The BSA-coated and CML particles adhere to the stiff fibrin network and are completely immobile within the resolution of the measurement; circles indicate their static positions. By contrast, the PEG-coated particles are resistant to the nonspecific protein adsorption and remain mobile with trajectories that resemble random walks.

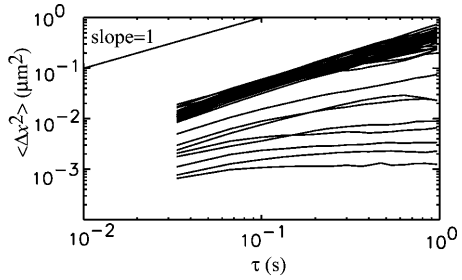

FIGURE 4 A sampling of the mean-squared displacements of individual PEG-coated particles moving in a fibrin network. Most particles diffuse, but some are locally constrained, leading to a plateau in their MSDs at long lag times.

Unlike the measurements of fibrin, we observe no measurable difference between the value of $\langle \Delta x_p^2 \rangle$ for the BSA- and PEG-coated particles, suggesting that the binding affinity of actin to the particles is weak in comparison to fibrinogen. Overall, the effect of varying surface chemistry for entangled actin solutions is small.

One- and two-particle microrheology measurements of F-actin/scruin networks

We measure only weak effects of particle surface modifications in pure actin solutions; however, physiological actin networks are stiffened by actin-binding proteins that cross-link, bundle, and nucleate filaments; moreover, actin networks in cells form in the presence of numerous globular proteins in the cytosol, as well as other cytoskeletal filaments (Alberts et al., 2002). Actin-binding proteins may display a stronger binding affinity for surfaces, leading to more striking differences in the mobility of particles with different surface modifications, and complicating the interpretation of particle tracking measurements in physiologically relevant

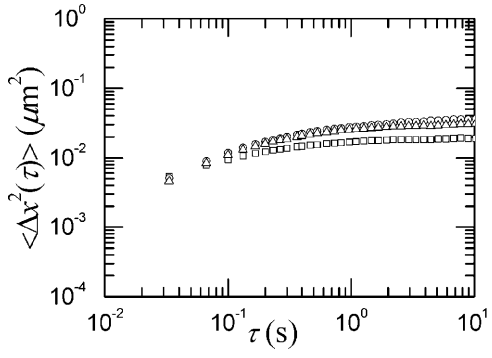

FIGURE 5 Ensemble averaged mean-squared displacements of 1.0-μm CML (□), BSA-coated (○), and PEG-coated (△) particles in an entangled F-actin solution. There is measurable decrease in the plateau value of the MSD of the CML particles as compared to those of the BSA- or PEG-coated particles; however, the overall effect is small, suggesting that the binding affinity of actin to bare CML particle surfaces is weak. We observe no difference between the plateau value of the MSDs for the BSA- and PEG-coated tracers.

actin gels and cytoplasm (McGrath et al., 2000). To further investigate these effects, we compare the movements of 1.0-μm CML, and BSA- and PEG-coated particles in F-actin networks that are cross-linked and bundled by the actin-bundling protein scruin. Scruin is found in the acrosomal bundle of horseshoe crab sperm, where it decorates individual actin filaments at a 1:1 stoichiometric ratio (Schmid et al., 1995). In vivo, scruin-scruin interactions align F-actin in a tight parallel array of neighboring filaments. In vitro, actin-scruin composite networks are used as model systems to investigate the mechanics and microstructure of cross-linked F-actin gels; in this case, the ratio of scruin to G-actin, R, is varied from 1:30 to 1 (J. Shin, M. Gardel, L. Mahadevan, P. Matsudaira, and D. Weitz, unpublished). Over these ratios, scruin serves to both cross-link and bundle actin filaments into a three-dimensional network. For small R, infrequent scruin-scruin interactions cross-link neighboring actin filaments that remain randomly oriented without promoting bundle formation. The network structure is only slightly perturbed from that of a purely entangled actin network, and is characterized by a mesh size in microns $\xi = 0.3/\sqrt{c_A}$, where c_A is the concentration of actin in mg/mL (Schmidt et al., 1989). At larger R, bundles form and as R is increased for a constant actin concentration, the bundle thickness increases, leading to a concomitant increase in the mesh size. Independent measurements have shown that for R ranging from 1:30 to 1, ξ varies from $\sim$0.5 μm to 8 μm (J. Shin et al., unpublished).

To investigate the role of scruin in the surface interactions between the tracer colloids and the gel, and to study the transition from a weakly cross-linked to a highly bundled network, we embed CML and BSA- and PEG-coated particles into the composite actin-scruin networks and observe the resultant particle displacements. In contrast to the solutions of purely entangled F-actin, we see dramatic differences in both the magnitude and time dependence of the MSDs of particles with different surface modifications. At the lowest concentration of cross-linkers, R = 1:30, the CML particles aggregate and no single tracers are observed, precluding measurements of particle dynamics. At higher cross-linker densities, this aggregation worsens and the CML particles form large clumps that sediment out of solution. By contrast, the BSA- and PEG-coated particles remain dispersed, consistent with their ability to better resist protein adsorption compared to unmodified spheres.

To further investigate the effect of surface chemistry on particle dynamics, we examine the MSDs of the BSA- and PEG-coated particles at different scruin/actin ratios. The concentration of actin is fixed at 11.9 μM (0.5 mg/mL), and the amount of scruin is varied to achieve the desired stoichiometric ratio. As shown in Fig. 6, for each R, the MSD of the BSA-coated particles (*solid symbols*) increases at short lag times, and saturates at a plateau value $\langle \Delta x_p^2 \rangle$ at $\sim \tau$ = 0.3 s; the value of $\langle \Delta x_p^2 \rangle$ decreases as the cross-linker density is increased from R = 1:30 (*solid squares*), to R = 1:15 (*solid circles*), to R = 1:5 (*solid triangles*). By contrast, the

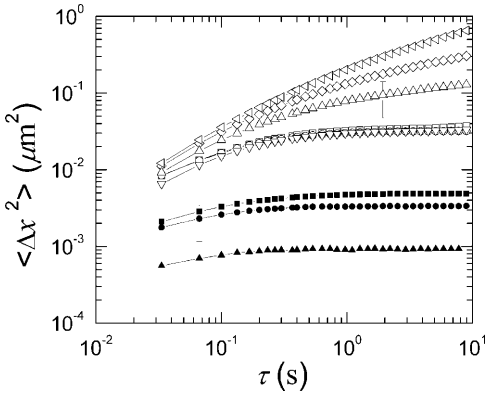

FIGURE 6 The ensemble averaged MSDs for BSA-coated particles (*solid symbols*) and PEG-coated particles (*open symbols*) moving in actin networks cross-linked and bundled with the actin-binding protein scruin, at various ratios of scruin/actin: $R = 1{:}30$ (□), 1:15 (○), 1:10 (▽), 1:5 (△), 1:2.5 (◇), and 1 (◁). Representative error bars are shown for each surface coating. The BSA-coated particles are constrained for each R, reaching a plateau $\langle \Delta x_p^2 \rangle$ that decreases with increasing amounts of scruin. The ensemble averaged MSDs for PEG-coated particles show a completely different trend for R ranging from 1:30 to 1. At the lower concentrations of cross-linkers, the particles are constrained; however, the particle mobility increases with increasing amounts of scruin, until at $R = 1$, the particles are nearly diffusive at short lag times.

PEG-coated particles (*open symbols*) show a completely different trend. At the lowest cross-linker density, $R = 1{:}30$ (*open squares*), the MSD saturates to a plateau value by a lag time of ~0.5 s; however, this value is more than five times larger than the plateau value observed with the BSA-coated particles at the same R. When the amount of scruin is increased slightly to $R = 1{:}15$ (*open circles*) and $R = 1{:}10$ (*downward open triangles*), there is no change in the MSDs of the PEG-coated particles despite the threefold change in cross-linker concentration. At higher cross-linker densities of $R = 1{:}5$ (*upward open triangles*), or greater, the ensemble-averaged MSD no longer reaches a true plateau, and the value of the MSD at long lag times is larger than that of particles moving in less cross-linked samples or the purely entangled F-actin solutions. At the highest cross-linker density of $R = 1$ (*leftward open triangles*), the MSD is nearly linear at short lag times. From this short time data, we calculate $\eta \approx 3$ mPa-s, similar to the viscosity of the background aqueous fluid, which we independently measure to be ~1 mPa-s.

The differences in the movements of the BSA-coated and PEG-coated particles reflect the differences in their protein-binding capacities, and demonstrate our ability to differentially probe a heterogeneous network using particles with carefully chosen surface modifications. The BSA-coated particles, although better able to resist protein adsorption than the bare CML spheres, are still somewhat ''sticky'' and adhere to the network; as a result, their movements reflect the thermal fluctuations of the polymer strands of the network. As we increase the amount of scruin, the average bundle diameter d increases, causing an increase in the bending modulus B of the bundled actin strands; for thin isotropic rods, $B \sim d^4$. Because the BSA-coated particles adhere to these bundles, they are sensitive to changes in local stiffness and move less with increasing amounts of scruin. By contrast, the protein-resistant PEG-coated particles are less likely to adhere to the network, and are instead merely constrained by the elastic cage formed by the surrounding polymer strands. At low and intermediate scruin concentrations, we observe no change in the plateau value of the MSD measured by the PEG-coated particles with increasing amounts of scruin, indicating little change in the local microenvironment. At larger concentrations of scruin, ξ increases beyond the fixed particle radius, allowing the PEG-coated particles to move more.

Because we measure similar dynamics for the BSA- and PEG-coated particles in pure entangled actin networks, we surmise that the differences we observe in the actin-scruin networks arise because the BSA-coated particles bind to scruin. This suggests that the BSA-coated particles are preferentially distributed to the scruin-rich regions of the gel, or alternatively that the BSA-coated particles recruit scruin to their surfaces, thereby altering the distribution of cross-linkers in the sample. By increasing the effective concentration of cross-linkers near the tracer surface, the BSA-coated beads create locally stiffer, more cross-linked regions of the gel near the particles, causing a reduction in the amplitude of their thermal fluctuations. By contrast, the PEG-coated particles resist the adsorption of scruin and are more randomly distributed among the native mechanical microenvironments of the gel. The possibility that there is a differential distribution of partially sticky and inert tracers in different mechanical microenvironments of the network is supported by the differences in $\langle \Delta x_p^2 \rangle$ for the BSA- and PEG-coated particles at low and intermediate scruin concentrations. We find that $\langle \Delta x_p^2 \rangle$ for the PEG-coated particles is a factor of 5–10 greater than that of the BSA-coated tracers in this regime where particles with both surface modifications are constrained by the network. Alternatively, it has been suggested that during the initial stages of gelation, before a percolated network has formed, nonbinding particles will migrate to the weaker regions of heterogeneous gels as this separation maximizes particle motions and thus is entropically favored (McGrath et al., 2000). We are unable to experimentally distinguish among these possibilities, or precisely interpret $\langle \Delta x_p^2 \rangle$ for the constrained particles in these composite networks.

To further explore these differences and reveal the underlying polymer dynamics, we use two-particle microrheology to measure the long wavelength fluctuations of the actin-scruin networks and determine the bulk viscoelastic response. For a network with $R = 1{:}30$, we observe a slight difference between the two-particle MSDs measured with the BSA-coated particles (*solid symbols*) and PEG-coated tracers (*open symbols*), as shown in Fig. 7 *A*; however, this

difference is significantly smaller than that measured with the one-particle MSDs, and is within the sample/sample variation. For a more strongly cross-linked network with $R = 1{:}15$, we measure a small decrease in the two-particle MSDs as compared to the data for $R = 1{:}30$, and good agreement between the data for the BSA- and PEG-coated particles as shown in Fig. 7 *B*. In all cases, the two-particle MSDs plateau at long lag times, and the plateau values for $\langle \Delta r^2(\tau) \rangle_D$ are lower than those measured by the one-particle techniques using either the BSA- or PEG-coated particles. Furthermore, we find that the two-particle analysis eliminates virtually all the differences between the BSA- and PEG-coated tracers. This suggests that although there are local differences in the coupling of the BSA- and PEG-coated particles to the network that give rise to differences in the one-particle MSDs, the particles do not induce large length scale inhomogeneities; moreover, the macroscopic stress relaxation measured by the two particle types is similar. To our knowledge, this is the first demonstration that two-particle microrheology methods successfully eliminate the local variations in mechanical response caused by differences in tracer surface chemistry.

Interestingly, for both samples, the two-particle MSD calculated from the data for the PEG-coated particles is noisier than that calculated using the data from the BSA-coated particles. In both cases, the particle dynamics are a superposition of local fluctuations, which are uncorrelated and unrelated to the long wavelength polymer fluctuations, and long wavelength modes due to the thermal fluctuations of the network itself, which lead to the correlated motions measured by the two-particle technique. Because the BSA-coated particles are physically coupled to the polymer filaments, a greater proportion of their Brownian dynamics reflects the fluctuations of the network. By contrast, the PEG-coated particles are less likely to bind to the network, and a smaller proportion of their Brownian motion reflects the correlated motions. This leads to a much poorer signal/noise ratio for the PEG-coated particles than for the BSA-coated particles, leading to noisier data in the two-particle MSD.

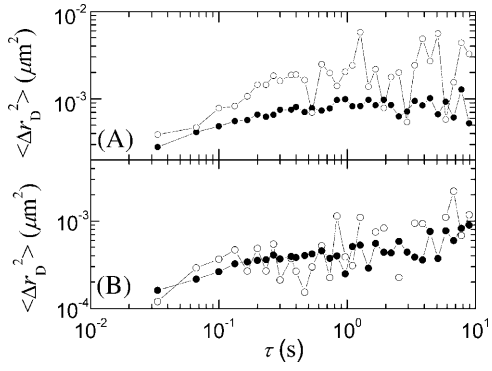

FIGURE 7 Two-particle mean-squared displacements for composite actin-scruin networks with (*A*) $R = 1{:}30$ and (*B*) $R = 1{:}15$; ~70 particles are included in this calculation. The long wavelength elastic modes are unaffected by local coupling of the particles to the network, and differences between the BSA-coated particles (*solid symbols*) and PEG-coated particles (*open symbols*) measured with one-particle techniques are eliminated. In all cases, the MSDs show a plateau at long lag times, and the plateau values of $\langle \Delta x_p^2 \rangle$ are significantly smaller than those measured by one-particle techniques.

SUMMARY

The examples of the fibrin, F-actin, and F-actin-scruin composite networks illustrate the rich information about local viscosity, elasticity, and microstructure available at a range of length scales with multiple particle tracking measurements, and demonstrate the challenges of interpreting particle movements in complex heterogeneous biomaterials. To achieve the full potential of these methods, the delicate interactions between the embedded probe colloids and the biopolymer networks must be understood and controlled. In particular, to understand the interplay between mechanics and structure in complex biomaterials, and to address important biological questions in vivo, it is critical to identify which aspect of the multi-component system is being probed.

In this article, we employ two types of particles with commonly used surface modifications, CML particles, and CML particles that have been coated with physisorbed BSA, and compare their adsorption properties and mobility to those of novel PEG-coated tracers. The binding capacity of the particles varies depending on the biopolymer we probe; however, in all cases, we find the CML particles adsorb the most protein, whereas the PEG-coated particles adsorb the least. Moreover, we find a correlation between increased protein binding capacity and decreased particle mobility. Thus, differences in particle dynamics measured with multiple particle tracking techniques may reflect differences in the particles' adsorption characteristics, as well as differences the local viscoelastic response or changes in local microstructure. When probing a new material, a careful study of the effect of both particle size and surface chemistry is absolutely required for the proper interpretation of multiple particle tracking experiments.

We have further demonstrated that binding and non-binding particles are sensitive to different physical properties of heterogeneous networks. Our measurements of particle displacements in fibrin networks and cross-linked and bundled actin gels suggest that particles that are weakly bound to the network are sensitive to changes in local stiffness but not microstructure, whereas the protein resistant PEG beads are sensitive to changes in viscosity and mesh size and less sensitive to changes in elastic modulus. Thus, judicious choice of colloid surface chemistry should allow us to selectively probe these different material properties of complex biomaterials. For two-particle microrheology measurements, differences arising from surface chemistry are eliminated, but the signal/noise ratio of the measurement increases when tracers adhere to the network. In cases such

as this, where a small amount of adsorption is desired, the uncontrolled synthesis, ill-defined characterization, and short shelf-life of the BSA-coated particles may be impractical. With slight modifications to the protocol described here, it is possible to create designer particles with dense methoxy-terminated PEG brushes that prevent nonspecific adsorption, but bind to a particular target protein by the addition of a small number of reactive PEG chains with terminal groups that present an antibody or other specific linkage (Lahiri et al., 1999). In addition to providing surfaces with tunable adsorption properties, such designer particles will allow mechanical measurements of a single component of a complex composite structure, such as in the cytoplasm of living cells.

This work was supported in part by grants from the National Science Foundation (DMR-0243715), the Materials Research Science and Engineering Center through the auspices of the National Science Foundation (DMR-0213805), and the National Aeronautics and Space Administration (NAG3-2284).

The authors also gratefully acknowledge support from the National Science Foundation Graduate Research Fellowship (J.H.S.), Lucent Graduate Research Program for Women Fellowship (M.L.G.), and Howard Hughes Medical Institute Predoctoral Fellowship (Z.E.P.). We thank J. Weitz, J. Rischke, and A. Lazier (McMaster University, Hamilton, Canada) for supplying the fibrin and thrombin and for technical support in handling these gels, E. Sackmann and A. R. Bausch (Technical University, Munich, Germany) for supplying the actin samples, G. Waller (Whitehead Institute for Biomedical Research, Cambridge, MA) for providing technical assistance in scruin purification, and J. Jiang and X. Qian (Dept. of Chemistry and Chemical Biology, Harvard University, Cambridge, MA) for useful discussions, insights, and technical advice.

REFERENCES

Alberts, B., A. Johnson, J. Lewis, M. Raff, K. Roberts, and P. Walter. 2002. Molecular Biology of the Cell. Garland, New York.

Alcantar, N. A., E. S. Aydil, and J. N. Israelachvili. 2000. Polyethylene glycol-coated biocompatible surfaces. *J. Biomed. Mater. Res.* 51:343–351.

Amblard, F., A. C. Maggs, B. Yurke, A. N. Pargellis, and S. Leibler. 1996a. Subdiffusion and anomalous local viscoelasticity in actin networks. *Phys. Rev. Lett.* 77:4470–4473.

Amblard, F., B. Yurke, A. Pargellis, and S. Leibler. 1996b. A magnetic manipulator for studying local rheology and micromechanical properties of biological systems. *Rev. Sci. Instrum.* 67:818–827.

Boal, D. 2002. Mechanics of the Cell. Cambridge University Press, Cambridge.

Bradford, M. M. 1976. Rapid and sensitive method for quantitation of microgram quantities of protein utilizing the principle of protein-dye binding. *Anal. Chem.* 72:248–254.

Chapman, R. G., E. Ostuni, L. Yan, and G. M. Whitesides. 2000. Preparation of mixed self-assembled monolayers (SAMs) that resist adsorption of proteins using the reaction of amines with a SAM that presents interchain carboxylic anhydride groups. *Langmuir.* 16:6927–6936.

Chen, D. T., E. R. Weeks, J. C. Crocker, M. F. Islam, R. Verma, J. Gruber, A. J. Levine, T. C. Lubensky, and A. G. Yodh. 2003. Rheological microscopy: local mechanical properties from microrheology. *Phys. Rev. Lett.* 90:108301.

Chirakul, P., V. H. Pérez-Luna, H. Owen, G. P. López, and P. D. Hampton. 2002. Synthesis ad characterization of amine-terminated self-assembled monolayers containing diethylene glycol linkages. *Langmuir.* 18:4324–4330.

Clark, R. A. F. 2001. Fibrin and wound healing. *Ann. N. Y. Acad. Sci.* 936:355–367.

Crocker, J. C., and D. G. Grier. 1996. Methods of digital video microscopy. *J. Colloid Interface Sci.* 179:298–310.

Crocker, J. C., M. T. Valentine, E. R. Weeks, T. Gisler, P. D. Kaplan, A. G. Yodh, and D. A. Weitz. 2000. Two-point microrheology of inhomogeneous soft materials. *Phys. Rev. Lett.* 85:888–891.

Dasgupta, B. R., S.-Y. Tee, J. C. Crocker, B. J. Frisken, and D. A. Weitz. 2001. Microrheology of polyethylene oxide using diffusing wave spectroscopy and single scattering. *Phys. Rev. E.* 65:051505.

de Gennes, P. G. 1987. Polymers at an interface: a simplified view. *Adv. Colloid Interface Sci.* 27:189–209.

De Sousa Delgado, A., M. Léonard, and E. Dellacherie. 2001. Surface properties of polystyrene nanoparticles coated with dextrans and dextran-PEO copolymers. Effect of polymer architecture on protein adsorption. *Langmuir.* 17:4386–4391.

Doolittle, R. F. 1981. Fibrinogen and fibrin. *Sci. Am.* 245:126–135.

Gardel, M. L., M. T. Valentine, J. C. Crocker, A. R. Bausch, and D. A. Weitz. 2003. Microrheology of entangled F-actin solutions. *Phys. Rev. Lett.* 91:158302.

Gittes, F., and F. C. MacKintosh. 1998. Dynamic shear modulus of a semi-flexible polymer network. *Phys. Rev. E.* 58:R1241–R1244.

Gittes, F., B. Schnurr, P. D. Olmsted, F. C. MacKintosh, and C. F. Schmidt. 1997. Microscopic viscoelasticity: shear moduli of soft materials determined from thermal fluctuations. *Phys. Rev. Lett.* 79:3286–3289.

Harder, P., M. Grunze, R. Dahint, G. M. Whitesides, and P. E. Laibinis. 1998. Molecular conformation in oligo(ethylene glycol)-terminated self-assembled monolayers on gold and silver surfaces determines their ability to resist protein adsorption. *J. Phys. Chem. B.* 102:426–436.

Haynes, C. A., and W. Norde. 1994. Globular proteins at solid/liquid interfaces. *Colloid. Surface. B.* 2:517–566.

Hough, L. A., and H. D. Ou-Yang. 1999. A new probe for mechanical testing of nanostructures in soft materials. *J. Nanoparticle Res.* 1:495–499.

Howard, J. 2001. Mechanics of Motor Proteins and the Cytoskeleton. Sinauer, Sunderland, MA.

Jeon, S. I., J. H. Lee, J. D. Andrade, and P. G. de Gennes. 1991. Protein surface interactions in the presence of polyethylene oxide. 1. Simplified theory. *J. Colloid. Interface Sci.* 142:149–166.

Jones, J. D., and K. Luby-Phelps. 1996. Tracer diffusion through F-actin: effect of filament length and cross-linking. *Biophys. J.* 71:2742–2750.

Keller, M., J. Schilling, and E. Sackmann. 2001. Oscillatory magnetic bead rheometer for complex fluid microrheometry. *Rev. Sci. Instrum.* 72:3626–3634.

Krall, A. H., and D. A. Weitz. 1998. Internal dynamics and elasticity of fractal colloidal gels. *Phys. Rev. Lett.* 80:778–781.

Lahiri, J., L. Issacs, J. Tien, and G. M. Whitesides. 1999. A strategy for the generation of surfaces presenting ligands for studies of binding based on an active ester as a common reactive intermediate: a surface plasmon resonance study. *Anal. Chem.* 71:777–790.

Levine, A. J., and T. C. Lubensky. 2000. One- and two-particle microrheology. *Phys. Rev. Lett.* 85:1774–1777.

Liu, J., L. M. Gan, C. H. Chew, C. H. Quek, H. Gong, and L. H. Gan. 1997. The particle size of latexes from dispersion polymerization of styrene using poly(ethylene oxide) macromonomer as a polymerizable stabilizer. *J. Appl. Polym. Sci.* 35:3575–3583.

Luby-Phelps, K. 2000. Cytoarchitecture and physical properties of the cytoplasm: volume, viscosity, diffusion, intracellular surface area. *Int. Rev. Cytol.* 192:189–221.

Maggs, A. C. 1997a. Micro-bead mechanics with actin filaments. *Phys. Rev. E.* 57:2091–2094.

Maggs, A. C. 1997b. Two-plateau moduli for actin gels. *Phys. Rev. E.* 55:7396–7400.

Mason, T. G., K. Ganesan, J. H. Van Zanten, D. Wirtz, and S. C. Kuo. 1997a. Particle tracking microrheology of complex fluids. *Phys. Rev. Lett.* 79:3282–3285.

Mason, T. G., H. Gang, and D. A. Weitz. 1997b. Diffusing-wave spectroscopy measurements of viscoelasticity of complex fluids. *J. Opt. Soc. Am.* 14:139–149.

Mason, T. G., and D. A. Weitz. 1995. Optical measurements of the frequency-dependent linear viscoelastic moduli of complex fluids. *Phys. Rev. Lett.* 74:1250–1253.

McGrath, J. L., N. J. Eungdamrong, C. I. Fisher, F. Peng, L. Mahadevan, T. J. Mitchison, and S. C. Kuo. 2003. The force-velocity relationship for the actin-based motility of *Listeria* monocytogenes. *Curr. Biol.* 13:329–332.

McGrath, J. L., J. H. Hartwig, and S. C. Kuo. 2000. The mechanics of F-actin microenvironments depend on the chemistry of probing surfaces. *Biophys. J.* 79:3258–3266.

Morse, D. C. 1998. Viscoelasticity of concentrated isotropic solutions of semiflexible polymers. *Macromolecules.* 31:7030–7067.

Ostuni, E., R. G. Chapman, R. E. Holmlin, S. Takayama, and G. M. Whitesides. 2001. A survey of structure-property relationships of surfaces that resist the adsorption of protein. *Langmuir.* 17:5605–5620.

Prime, K. L., and G. M. Whitesides. 1993. Adsorption of proteins onto surfaces containing end-attached oligo(ethylene oxide): a model systems using self-assembled monolayers. *J. Am. Chem. Soc.* 115:10714–10721.

Prime, K. L., and G. M. Whitesides. 1991. Self-assembled organic monolayers: model systems for studying adsorption of proteins at surfaces. *Science.* 252:1164–1167.

Schmid, M. F., J. M. Agris, J. Jakana, P. Matsudaira, and J. W. Chiu. 1995. Three-dimensional structure of a single filament in the Limulus acrosomal bundle: scruin binds to homologous helix-loop-beta motifs in actin. *J. Cell Biol.* 124:341–350.

Schmidt, C. F., M. Baermann, G. Isenberg, and E. Sackmann. 1989. Chain dynamics, mesh size, and diffusive transport in networks of polymerized actin: a quasielastic light scattering and microfluorescence study. *Macromolecules.* 22:3638–3649.

Schmidt, F. G., F. Ziemann, and E. Sackmann. 1996. Shear field mapping in actin networks by using magnetic tweezers. *Eur. Biophys. J.* 24:348–353.

Shay, J. S., R. J. English, R. J. Spontak, C. M. Balik, and S. A. Khan. 2000. Dispersion polymerization of polystyrene latex with novel grafted poly(ethylene glycol) macromers in 1-propanol/water. *Macromolecules.* 33:6664–6671.

Shay, J. S., S. R. Raghavan, and S. A. Khan. 2001. Thermoreversible gelation in aqueous dispersions of colloidal particles bearing grafted poly(ethylene oxide) chains. *J. Rheol.* 45:913–927.

Sun, S., M. Footer, and P. Matsudaira. 1997. Modification of Cys-837 identifies an actin-binding site in the beta propeller protein scruin. *Mol. Biol. Cell.* 8:421–430.

Tilney, L. G., M. S. Tilney, and G. M. Guild. 1996. Formation of actin filament bundles in the ring canals of developing Drosophila follicles. *J. Cell Biol.* 133:61–74.

Valentine, M. T., L. E. Dewalt, and H. D. Ou-Yang. 1996. Forces on a colloidal particle in a polymer solution: a study using optical tweezers. *J. Phys. Condens. Matter.* 8:9477–9482.

Valentine, M. T., P. D. Kaplan, D. Thota, J. C. Crocker, T. Gisler, R. K. Prud'homme, M. Beck, and D. A. Weitz. 2001. Investigating the microenvironments of inhomogeneous soft materials with multiple particle tracking. *Phys. Rev. E.* 64:061506.

Valiokas, R., S. Svedham, M. Östblom, S. C. T. Svensson, and B. Liedberg. 2001. Influence of specific intermolecular interactions on the self-assembly and the phase behavior of oligo(ethylene glycol)-terminated alkanethiolates on gold. *J. Phys. Chem. B.* 105:5459–5469.

Weisbecker, C. S., M. V. Merritt, and G. M. Whitesides. 1996. Molecular self-assembly of aliphatic thiols on gold colloids. *Langmuir.* 12:3763–3772.

Wong, I. Y., M. L. Gardel, D. R. Reichman, E. R. Weeks, M. T. Valentine, A. R. Bausch, and D. A. Weitz. 2004. Anomalous diffusion probes microstructure dynamics of entangled F-actin networks. *Phys. Rev. Lett.* 92:178101.

Ziemann, F., J. Rädler, and E. Sackmann. 1994. Local measurements of viscoelastic moduli of entangled actin networks using an oscillating magnetic bead micro-rheometer. *Biophys. J.* 66:2210–2216.